Multi-Objective Optimization of Aircrafts Family at Conceptual Design Stage

Thierry Druot[⋆], *Stephane Alestra*[*],
Christophe Brand[†], *Sergey Morozov*[‡]

[⋆] *AIRBUS, EIX, thierry.druot@airbus.com*
[*] *DATADVANCE, stephane.alestra@datadvance.net*
[†] *DATADVANCE, christophe.brand@datadvance.net*
[‡] *DATADVANCE, sergey.morozov@datadvance.net*

Abstract

We consider conceptual design problem of a family of aircrafts of different capacities yet having maximum number of elements in common to reduce maintenance and operational costs. Each family member has its own operational requirements and cost criteria, which makes the family selection a multi-criteria equality constrained optimization problem. The conceptual design task supplemented with semi-empirical models for geometry, aerodynamics, weights and performances is successfully solved using MACROS software developed by DATADVANCE. We managed to greatly improve considered performance measures and quantitatively describe the whole variety of optimal non-dominated solutions.

1. Introduction

Conceptual Design is the very first step of aircraft design project during which the general arrangement of the aircraft is defined, selecting the overall positions and shapes of various components, as well as the most suitable technologies. These choices are crucial for the project progress and its profitability while wide range of uncertainty is attached to most of the assumptions and evaluation processes. The economical viability of a given project of a new airplane is even more difficult to assess as it has to be put in the perspective of the competition landscape.

Actually, in order to make the largest feedback on R&D investment and to maximize the product attractiveness it is usual to consider the production of a family of aircrafts of different capacities rather than an aircraft alone. With highly similar products, this allows covering a more important market part than a single aircraft. All the members of this family of aircrafts have different fuselage lengths and characteristic weights but they have in common a maximum number of elements which may reduce drastically airliners maintenance and operational costs.

Generally, there is a central configuration from which are taken the other members of the family. These are usually realized adding or removing fuselage sections, adapting engine rating thrusts or changing engines and optimizing structural reinforcements of a limited number of components. This will result in airplanes with different nominal ranges and characteristic weights. To give an example, Fig. 1 shows the market place covered by a family of three aircrafts. It is important to notice that each aircraft in this type of graphic is facing existing, or projected, competitor airplanes.

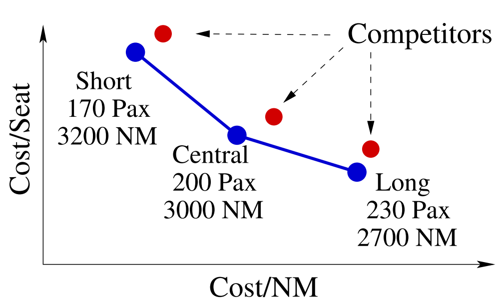

Figure 1: Market place covered by 3-aircraft family.

Being inside slightly different market segments, each member of the family has its own operational requirements but also its own cost criteria which makes the family optimization a basic multi-criteria problem. Some of the design parameters (as the wing design parameters) are common to all members of the family but some others (as the engine maximum thrust) are specific to each member. Due to coupling through family parameters, any design parameter (family or member specific) can be sized by any member specific constraints. To complicate a little bit the picture, it is usual to put in concurrence several criteria such as Cash Operating Cost (COC), Maximum Take Off Weight (MTOW) and Mission Fuel (FUEL) in order to assess some robustness of the optimum.

Due to business strategic considerations, aircraft family optimization requires that several possible solutions be exhibited in order to let freedom to decision making. The Pareto Front in the criteria space and its associated Pareto Set in the parameter space[1] is probably one of the most relevant mathematical tool to capture most of possible compromises.

The following study illustrates this approach. AIRBUS in-house simulation toolbox was used to evaluate design criteria and constraints. The toolbox is based on semi-empirical models covering all main physics that are interacting at conceptual design phase: geometry, aerodynamics, weights and performances. Implemented processes are classical and performed independently for each member of the family of three aircraft. These processes are coupled only through input design parameters and member specific constraints. MACROS Generic Tool for Optimization [3] was used to perform multi-objective optimization.

In section 2 we describe the formulation of the multi-objective optimization problem. Section 3 describes the details of MACROS multi-objective optimization algorithm. In section 4 we present results of optimization of family of aircrafts.

2. Problem Formulation

In the considered multi-objective optimization problem design variables are naturally structured: there are three different aircraft families "CENTRAL", "LONG" and "SHORT", each of which is characterized by three specific parameters: "MTOW" (Maximum TakeOff Weight), "MZFW" (Maximum Zero Fuel Weight) and "SLST" (See Level Specific Thrust). However, apparent symmetry of design types is broken for CENTRAL design: it additionally possesses "AR" (wing Aspect Ratio), "AREA" (wing area) and "BPR" (engine ByPass Ratio) design variables, which provide the interconnection between different families: in their absence the problem would break up into three independent models for each design type. In the sequel we abbreviate the names of all design parameters, for instance, "SHORT/MTOW" stands for SHORT design type MTOW variable. Each design variable is naturally bounded, there are *a priori* known attainable minimal/maximal values. Reference design point, also used as a starting point for optimization, corresponds to one of the currently considered at AIRBUS family of future aircrafts.

The problem is characterized by nine performance criteria (objective functions) to be minimized and they follow the same symmetry pattern. For each design type we consider three performance measures: "COC" (operational cost), "FUEL" (fuel consumption) and "MTOW" (maximum takeoff weight)[2]. Problem is subjected to 33 non-linear constraints. Particular symmetry is also clearly visible among the imposed constraints: each design type possesses its own set 9 inequalities and 2 normalized to zero equalities.

To summarize: the problem design space is not large (N=12), but the prime difficulty is to consider many performance measures (K=9) simultaneously. We stress that such large number of objective functions is notoriously difficult to handle, we're not aware of any efficient optimization algorithm capable to deal with such cases. Moreover, imposed set of constraints (M=33 in total, six of which are equalities) utterly complicates the model and it becomes a real challenge to solve it.

3. Solution Methodology

This section succinctly describes optimization algorithms which were used to solve given problems. Consideration is indeed very brief, in a nutshell only, simply because it goes far beyond the scope of this paper to treat all subtleties of concrete algorithm implementation. Instead our primal goal is give a feeling of underlying ideas leaving aside all technicalities involved. We're in haste to add, however, that utilized algorithms are not experimental and are in production stage for several years already as a part of MACROS Generic Tool for Optimization (GTOpt) developed by DATADVANCE. Moreover, GTOpt itself is only one of many other Generic Tools available in MACROS and its front end named Problem Solving Environment (PSE), please refer to [3] for details and further references.

In sections 3.1 and 3.2 we describe a few algorithms aimed to discover nearest to current iterate (locally) Pareto optimal solutions. Then in Sec. 3.3 we discuss Pareto frontier local geometry, knowledge of which allows us to spread from already known optimal designs towards nearby other optimal solutions. Sections 3.4 and 3.5 provide summary of multi-objective optimization approach used in GTOpt, prime advantage of which is the ability to always stay close to optimal set. Note that this is not the only multi-objective optimization method available in MACROS, but essentially this one was used to solve the problem of aircraft family optimization.

To simplify presentation below it is convenient to introduce some notations. We say that particular constraint c^i and coordinate x^i is *lower-active* (*upper-active*) if its value equal to corresponding lower (upper) limit, $c^i = c^i_L (c^i = c^i_U)$

[1]Pareto optimal solutions are defined to be feasible designs at which none of performances could be further improved without sacrificing some others

[2]There is no name clash between MTOW objectives and MTOW design variables: these are identically the same quantities.

and $x^i = x^i_L (x^i = x^i_U)$, correspondingly. Union of indices of all lower- and upper-active constraints constitutes set of active constraints $\mathcal{A}$ and set of active box bounds $\mathcal{A}_b$. For each active constraint or box bound we also define corresponding sign s^i which is $+1$ for upper-active and is -1 for lower-active entries.

3.1 Optimal Descent

This is one of the basic algorithms needed in almost all other methods, its theoretical foundations can be found in Ref. [1]. Purpose is to estimate optimality of current iterate x_k in the context of multi-objective constrained problems. As a by product (if current iterate is not optimal) method allows to get the direction of optimal descent which is a direct analog of well known steepest descent direction in single-objective unconstrained case.

Mathematically the problem is formulated as follows. Given current feasible point x we would like to find (or ensure the absence of) direction d in N-dimensional design space such that d is descent direction for all objectives $d \cdot \nabla f^i \le 0, \quad i = 1, ..., K$ and it violates none of imposed bounds in linear approximation

$$c^j_L \le c^j + d \cdot \nabla c^j \le c^j_U, \quad j = 1, ..., M \qquad\qquad x^k_L \le x^k + d \le x^k_U, \quad k = 1, ..., N \tag{1}$$

Generically, if current iterate is not yet optimal there are a whole variety of solution to the above problem. In the case of single objective optimization this freedom is fixed by requirement to find direction of maximal objective decrease. In multi-objective situation we would like instead to maximally reduce all objectives. Leaving for a moment aside the feasibility considerations we therefore obtain auxiliary optimization problem

$$\min_d \max_i \; d \cdot \nabla f^i \qquad \Leftrightarrow \qquad \min_{d,t} \; t \quad \text{s.t.} \quad d \cdot \nabla f^i \le t \tag{2}$$

supplemented with the requirement $|d|_\infty \le 1$ (in principle, any other restriction on d norm could be used, but L_∞ norm leads to most simple formulation). Note that single objective $K = 1$ recipe $d = -\nabla f$ is a particular case of (2). Restoring requirements of feasibility we finally get the following linear optimization problem which determines direction of optimal descent:

$$\begin{array}{ll} \min\limits_{d,t} & t \\ \text{s.t.} & d \cdot \nabla f^i \le t \\ & s^j \, d \cdot \nabla c^j \le t \quad j \in \mathcal{A} \end{array} \qquad \forall k \;:\; d_k \in \begin{cases} [0:1] & x_k \text{ is lower-active} \\ [-1:0] & x_k \text{ is upper-active} \\ [-1:1] & \text{otherwise} \end{cases} \tag{3}$$

Note that appearance of t variable in active constraints related restrictions is a pure regularization, it account for missing constraints curvature information. Away from optimality it forces optimal descent direction to be slightly away from tangents to active constraints while near the optimal solution its effect disappears. In what follows we call optimal solution d of the problem (3) optimal descent and magnitude of corresponding optimal t value is called "optimal descent magnitude". Note that vanishing magnitude of optimal descent implies (local) optimality of considered point. Therefore linear problem (3) is an universal mean to measure optimality of current iterate.

Despite of apparent simplicity of the above construction there are a lot of complications which are especially relevant in multi-objective context. For instance, special care is needed when constraints matrix A of linear problem (3) turns to be rank-deficient. Real trouble related to weak Pareto optimality appears when particular objective gradients, say ∇f^{i0} is in null space of A: $\nabla f^{i0} \in \text{null}(A)$. In this case special type of matrix A reduction must be performed to catch proper descent and the convenient way to do so is to convert problem (3) into its dual formulation.

As it is usual with first order methods convergence to optimality might be slow when optimal descent is used in line-search like procedures. Particular manifestation of this is improper scaling of optimal descent: in formulation (3) d always has unit L_∞-norm and line search becomes quite expensive simply because there is no sensible prediction for the magnitude of the line step. The usual remedy known in the field of single-objective unconstrained optimization is to repeat derivation of optimal descent, but with second order information included at every step. Note that in constrained case Sequential Quadratic Programming (SQP) follows the same idea, but only partially (constraints are still considered in linear approximation, their curvatures enter the game rather indirectly via approximations to problem Lagrangian). What we get when second order information is included in derivation of optimal descent is the generalization of (Quasi-)Newton (QN) method to the case of multiple objective functions and constraints [2]. It is generically expected that methods based on QN descent are to be quadratically convergent and, in particular, produce well-scaled search direction d.

3.2 Multi-Objective Descent

It is apparent from the above presentation that procedures to obtain optimal and QN descent are universal and applicable to virtually all optimization problems, in particular, to constrained multi-objective ones. Therefore, we could almost verbosely translate this general scheme to the considered case, the only crucial distinction being in proper line step selection. Indeed, while in single-objective case there are a few efficient line search algorithms available, only Armijo-like line search rule is applicable in multi-objective context. Concretely, for $K > 1$ objective functions MO Armijo rule requires to satisfy usual Armijo criterion simultaneously for all objectives. Since point suitable for usual Armijo line search is guaranteed to exist for sufficiently small line coordinates, it follows that in case of multiple objective functions appropriate for MO Armijo criterion points could always be found in small vicinity of current iterate. On the other hand, Armijo rule is known as rather inefficient even in single-objective case, therefore the use of well scaled QN descent direction becomes particular important in multi-objective optimization.

From general point view MOPDescent algorithm implements multi-objective constrained programming functionality, where MO optimization is understood in local sense: purpose is to find nearest to current iterate Pareto optimal solution. Indeed, by construction MOPDescent finds only a single Pareto-optimal solution. On the other hand, the fact that it utilizes line search along optimal or QN descent direction almost guarantees that MOPDescent will find nearest to starting point optimal point. At least, MOPDescent has no built in mechanism or internal reasons to search for optimal set far away from initial position.

3.3 Multi-Objective Optimization

Algorithm described in this section implements multi-objective constrained programming functionality. Generic idea underlying considered method is to maximally avoid end-user functions evaluations away from Pareto frontier. Indeed, in our opinion the weakest point of most popular nowadays stochastic (genetic, in particular) approaches is that they spend almost all the time far away from optimal set trying to move whole bunch of points "simultaneously" towards Pareto frontier. At the same time, as we'll argue below, Pareto set in many cases possesses distinct geometrical properties which allow to identify it without the need to ever calculate anything away from frontier itself. In a nutshell, our algorithm first finds only a few optimal solutions and then performs something like diffusion along Pareto frontier. Qualitatively, the process is illustrated on Fig. 2, see below for detailed description.

To be concrete, let us assume that initial problem is smooth and that corresponding Pareto front consists of finite number of disjoint components each of which could locally be represented as a differentiable manifold. There are dozens of problems of pure mathematical and engineering origin which satisfy this assumption. However, it is worth emphasizing that there are indeed a variety of important problems which does not satisfy the above assumptions and for which our method is not directly applicable (at least not in its naive implementation).

In order to understand local geometry of Pareto optimal set it is enough to remind optimal descent construction of section 3.1. Namely, we noted before that magnitude of optimal descent is a natural measure of optimality of current iterate. Moreover, its vanishing value indicates that at least locally current point satisfies first order optimality conditions. It crucial here that the constraint $|d|_\infty \leq 1$ entering (2) was introduced in ad hoc manner, its sole purpose was to remove rescaling freedom $d \rightarrow \alpha\, d$ which makes (2) not well defined. The same effect could be achieved by introducing, e.g., $1/2\,|d|_2^2$ term in the objective function. Of course, away from optimality both optimal descent and descent magnitude would change upon this substitution, however, we're considering (almost) optimal position for which the difference between $|d|_\infty \leq 1$ constraint and $1/2\,|d|_2^2$ term in objective is irrelevant.

To simplify presentation let us consider unconstrained multi-objective context[3] for which dual formulation of (2) with added $1/2\,|d|_2^2$ term is easy to derive. Namely, one can show that optimal descent vector d and descent magnitude t are given by $d = -\sum_i \lambda_i^* \,\nabla f^i$, $t = -\frac{1}{2}|d|^2$ where dual variables λ^* solve the following quadratic problem

$$\min_\lambda \frac{1}{2}\,|\,\lambda_i\, \nabla f^i\,|^2 \qquad \text{s.t.} \qquad \sum_i \lambda_i = 1\,, \quad \lambda_i \geq 0 \tag{4}$$

with positive-semidefinite Hessian $G_{ij} = (\nabla f^i \cdot \nabla f^j)$. Optimality of considered point means that λ^* is the zero mode of G and in general case it is the only zero mode. What are the other eigenvectors $\lambda^{(\gamma)}$, $\gamma = 1, ..., K-1$ of G? In fact, one can easily show that each vector

$$t^\gamma = \mu_{(\gamma)}^{-1/2} \sum_i \lambda_i^{(\gamma)}\, \nabla f^i \tag{5}$$

is tangent to Pareto set at considered point and their union $\{t^\gamma, \gamma = 1, ..., K-1\}$ constitutes orthonormal basis in corresponding tangent plane. Here $\mu_{(\gamma)}$ are the eigenvalues of G, $G\lambda^{(\gamma)} = \mu_{(\gamma)}\,\lambda^{(\gamma)}$.

How above construction modifies in presence of active constraints? It turns out that modifications are rather simple. Let us denote by $P_{\mathcal{A}}$ linear $N \times N$ projector onto the space tangent to all currently active constraints (including active box bounds). Then constrained analog of (4) could be obtained upon substitution $\nabla f^i \longrightarrow P_{\mathcal{A}}\, \nabla f^i$.

[3] We'll indicate which modifications are needed (they are minimal, in fact) to capture constrained case as well.

How the knowledge of Pareto set local geometry helps to discover new Pareto optimal solutions? Idea is rather simple, consider infinitesimal shift (called "scattering" in what follows) from current optimal solution x^* along arbitrary tangent $x = x^* + \epsilon\, t^{(\gamma)}$. It is quite evident that optimality measure (magnitude of optimal descent) at x is of order $O(\epsilon)$. What remains to be done is to push x to true optimal position using, e.g., MOPDescent method of section 3.2. This approach is operational even for finite ϵ, but, of course, the amount of work needed to reach optimal set from x increases with increasing ϵ. Scattering and re-optimization steps are illustrated on Fig. 2 by the sequence of red (optimal) and blue (yet not optimized) points connected with black (scattering) and green (re-optimization) lines. Evidently, for sufficiently small scattering steps algorithm never leaves close vicinity of Pareto optimal solutions.

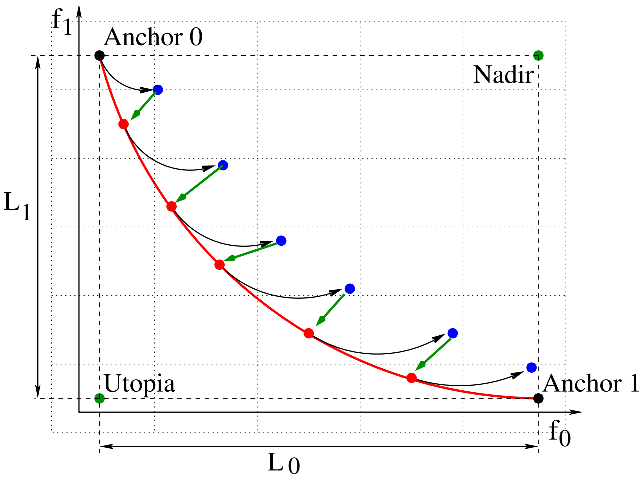

Figure 2: Qualitative illustration of Pareto front discovery algorithm (see text for details).

How to choose ϵ value in order to make the above approach practically sound? Surely, there is no unique solution, algorithm accepts the following strategy. We require end-user to provide a single parameter which specifies how many optimal points he/she would like to have on Pareto frontier at the end of multi-objective optimization. Note that this number is only approximate, actual amount of finally discovered optimal solutions crucially depends upon front geometry (which is yet unavailable). However, as on order of magnitude estimate this is perfectly acceptable. Then we need to roughly estimate extent of Pareto frontier along each axis in objective space. This could be done using conventional notions of anchors, nadir and utopia points (see below for details). User-given number of points together with estimated Pareto front bounding box allows to represent objective space as union non-overlapping equal-sized boxes. Then the ultimate goal of algorithm is to place at most one optimal solution into each box (of course, boxes could contain no optimal points at all which means that Pareto frontier does not pierce this particular box). This suggests the following policy to select proper value of ϵ parameter: it should be such that objective space points $f(x^*)$ and $f(x^* + \epsilon\, t^{(\gamma)})$ belong to neighboring boxes.

3.4 Anchors search

Purpose of this stage is to roughly estimate global geometry of Pareto frontier, namely, its extent along each objective space axis (global bounding box). Note that this does not mean that we will discover optimal solutions only within this bounding box. By definition i-th anchor point has minimal value of i-th objective (let it be $f^i_{*(i)}$) with no regard to all other objective values $f^j_{*(i)}$, $j \neq i$. However, at this point the problem of weak Pareto optimality comes into play. Namely, it might happen that keeping i-th objective at its minimal value we could still diminish some other objectives as well. Therefore, we formulate i-th anchor search problem, $i = 1, ..., K$, as follows: for all $k = 0, ..., K-1$ we sequentially solve

$$\min\ f^{(i+k) \bmod K} \qquad f^{(i+j) \bmod K} \leq f^{(i+j) \bmod K}_{*(i)} \qquad j = 0, ..., k-1 \tag{6}$$

to obtain i-th anchor point $\vec{f}^{(i)} = \{f^j_{*(i)}\,;\ j = 1, ..., K\}$. Utopia $\vec{f}^{min}$ and nadir $\vec{f}^{max}$ points

$$\vec{f}^{min} = \{\min_i\ f^j_{*(i)}\,;\ j = 1, ..., K\} \qquad \vec{f}^{max} = \{\max_i\ f^j_{*(i)}\,;\ j = 1, ..., K\} \tag{7}$$

naturally define Pareto frontier global bounding box (see Fig. 2), from which we derive the required objective space distance between optimal solutions to be produced.

3.5 Diffusion along Pareto Frontier

During the Pareto front discovery our algorithm keeps two set of points: i) not optimal set: candidate points obtained via scattering (see above) from optimal solution, which are generically do not satisfy optimality conditions; ii) optimal set: discovered so far optimal solutions. Right after anchor search stage all found anchor points are inserted into *both* sets. Moreover, to stabilize algorithm and to make it more robust any number of trial not optimal candidates could also be inserted into the first set. Then algorithm enters second iterative "diffusion" stage which could be summarized as follows (see Fig. 2 for illustration):

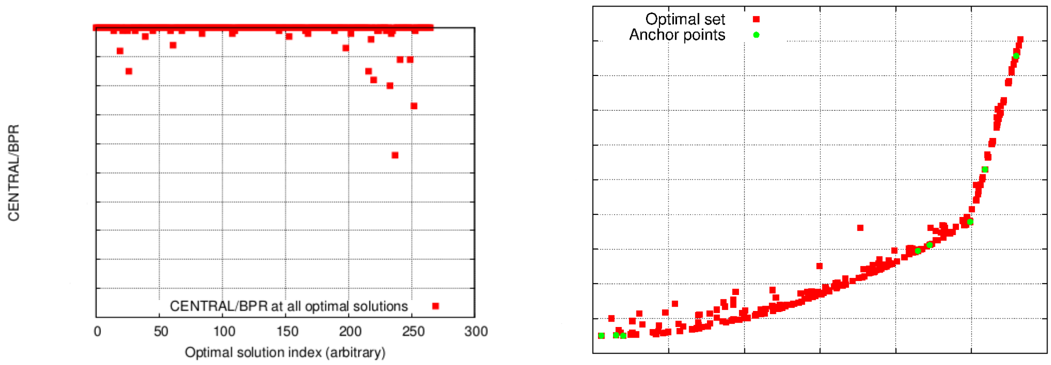

Figure 3: Left panel: bypass ratio (CENTRAL/BPR) design variable at all optimal solutions. Right panel: slice of Pareto set along CENTRAL/AR – CENTRAL/AREA coordinates.

1. Pick particular not optimal candidate point from not-optimal set and push it to optimality using MOPDescent method of section 3.2. If there are no more non-optimal candidates algorithm terminates.
2. Goto step 1 if just optimized point falls into vicinity of already known optimal solution (notion of "vicinity" is quantified by bounding box constructed previously).
3. Insert obtained solution into the optimal set and reconstruct Pareto front local geometry at this point to get complete basis $t^{(\gamma)}$ in corresponding tangent plane.
4. Perform scattering from current optimal solution to get new not optimal candidates to be inserted into non-optimal set. Namely, for each tangent direction $\pm\, t^{(\gamma)}$ we move along it until trial point goes beyond the bounding box centered at optimal solution in the objective space. Continue with next tangent direction in case we already have optimal solution or non-optimal candidate in the vicinity of trial point. Otherwise, insert trial into the set of non-optimal candidates.
5. Goto step 1.

4. Pareto Frontier Analysis

Multi-objective optimization algoritm, described in 3 and implemented in MACROS, was used to solve family of aircrafts optimization problem. In this section we present optimization results and describe the structure of obtain Pareto optimal solutions.

4.1 Qualitative Picture

For general "bird-eye" overview of Pareto frontier the most relevant quantities are the attained minimal values of each objective functions, the so called anchor points. Indeed, relative variation of k-th function among various anchors gives characteristic extent of Pareto frontier along k-th axis in objectives space. Already from the set of anchor points we conclude that Pareto frontier is very compact and that there are high correlations between objectives. Indeed, it is surprising that difference in each objective values at various anchors is much less than one percent in all cases. Taken at face value this means that the whole frontier collapses to almost one point, its extent in objective space is almost negligible compared to relevant characteristic scales. It is important to note that reduction of all objectives with respect to initial values is significant and is of order 10-20%. Therefore, at least at crude 'zero order' approximation Pareto front squeezes not only with respect to corresponding objective values but also with respect to corresponding amounts of improvement.

4.2 Quantitative Analysis

The particular advantage of our algorithm is its adaptiveness: method adjusts internal parameters in run-time and allows to see the structure of even almost squeezed optimal set. For instance, during the "diffusion" stage optimal set

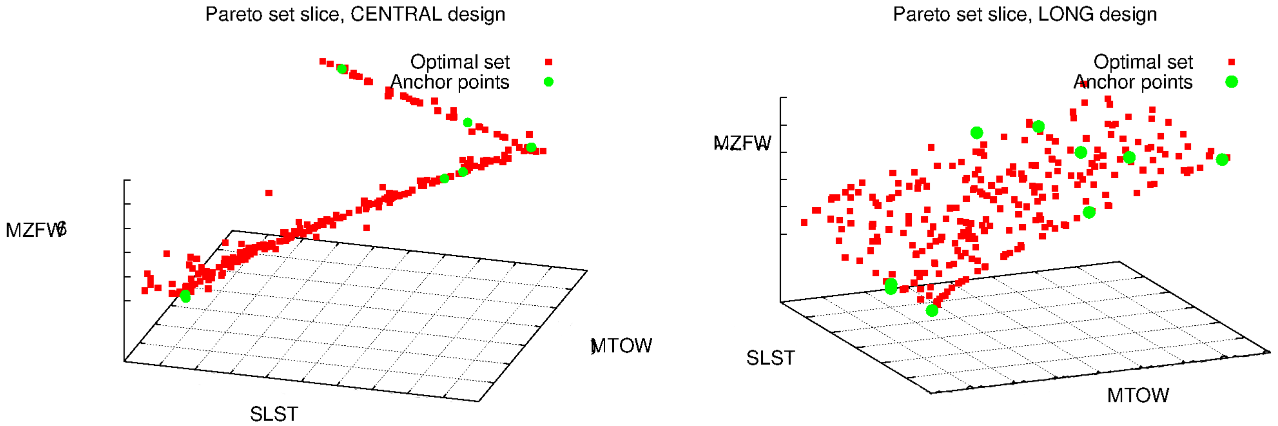

Figure 4: Pareto set three-dimensional slice along CENTRAL [left] and LONG [right] designs in (SLST)–(MTOW)–(MZFW) variables.

is reconstructed similarly to heat propagation on non-linear manifolds and it does not really matters how extended the front is. This allows us to conduct semi-quantitative analysis of the set of optimal solutions to be presented in this section. Note that due to confidentiality reasons we intentionally omit relevant numbers and scales in all figures.

Pareto Set

Numerically obtained Pareto optimal solutions is nothing but the sequence of triples $\{x_i, f_i, c_i\}$ representing particular optimal design point. From these numbers along it is very difficult to extract Pareto set as a piece-wise continuous manifold. The best we can currently do is to plot two- or three-dimensional slices of discretized Pareto set perhaps using some *a priori* provided hints on the nature of design variables. Fortunately, even this dumb analysis reveals quite non-trivial structure of the Pareto set.

First immediate observation is that bypass ratio variable (BPR) always stays at its maximal allowed value, its deviation from upper imposed bound is negligible, see Figure 3. Conclusion is that we could safely forget about BPR keeping it constant. Furthermore, we noted already that there is a particular symmetry among the design variables (see section 2), due to which it is natural to consider first the slices of Pareto set along (aspect ratio)-(wing area) coordinates (CENTRAL/AR-CENTRAL/AREA), Figure 3. Amusingly enough, for all possible values of remaining nine coordinates (BPR is frozen) Pareto set in CENTRAL/AR-CENTRAL/AREA plane looks almost one-dimensional, deviations being practically negligible.

Exploiting the symmetry of design variables we consider Pareto set slices along the coordinates (SLST)–(MTOW)–(MZFW), which are presented on Figure 4 for CENTRAL and LONG design types. Surprisingly, we see essentially two-dimensional structure of Pareto optimal solutions, which is confirmed by analogous plot for SHORT design type (not shown). Moreover, it seems that two-dimensional structure is entirely due to the particular SLST dependence: for both LONG and SHORT designs slices in (MTOW)–(MZFW) variables completely hide two-dimensional picture, Pareto set looks one-dimensional. This could only happens if the optimal set projected onto particular (SLST)–(MTOW)–(MZFW) triple is everywhere parallel to SLST axis. Note that this is in sharp contrast with CENTRAL design type properties. Overall conclusion of this rather dumb analysis is that Pareto set in the considered problem seems to be three-dimensional: *i*) In all slices perpendicular to LONG/SLST and SHORT/SLST optimal set looks one-dimensional; *ii*) Slicing along LONG/SLST, SHORT/SLST reveals that Pareto set is parallel to these axes.

We could readily confirm the above proposition with multiple plots of remaining slices. For instance, let us consider various three-dimensional slices taken for randomly chosen triple of design variables *excluding* LONG/SLST and SHORT/SLST parameters. As a matter of fact, in all these cases Pareto set looks like one-dimensional object. Contrary to that if we consider coordinate slices with either LONG/SLST or SHORT/SLST parameters *included* then optimal set appears as two-dimensional manifold. Moreover, we could also investigate three-dimensional slices along LONG/SLST, SHORT/SLST and any other coordinate: conclusion is that the apparent dimensionality of Pareto set is three in this case.

To summarize: Pareto set is likely to be a three-dimensional manifold with very specific structure: it goes in parallel to LONG/SLST and SHORT/SLST coordinate axis.

Pareto Front

Pareto front is clearly a derived quantity with respect to Pareto set, it is obtained by mapping Pareto set into objective space via given objective functions. In non-degenerate situation specific features of Pareto set imply similar

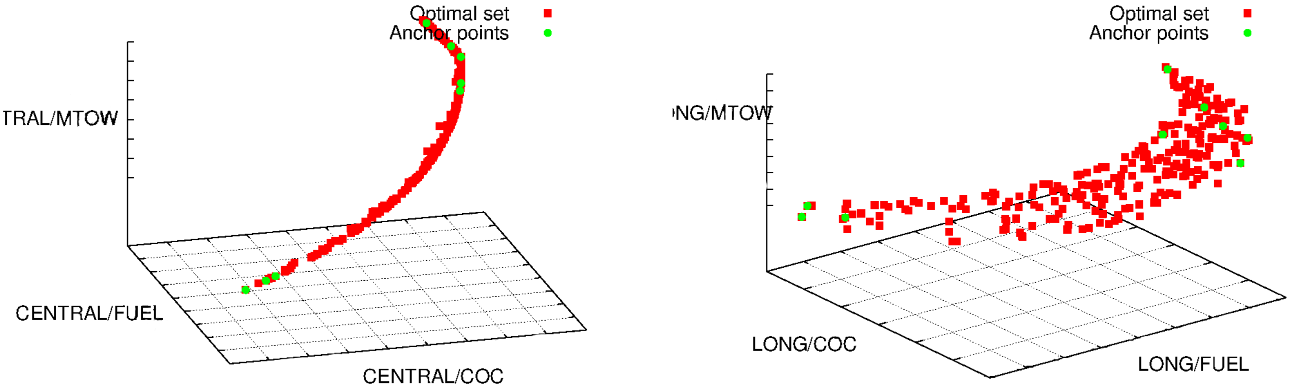

Figure 5: Pareto front projections onto coordinate triple (COC)–(FUEL)–(MTOW) for CENTRAL (left) and LONG (right) design type.

properties of Pareto front, however, we do know *a priori* that degeneracies are present in the considered problem and hence Pareto front is to be investigated independently. Due to the lack of convenient visualization tools we could only perform similar to above dumb analysis of Pareto front. Noted above symmetry of the problem greatly simplifies reasonable choice of objective functions to study in three-dimensional slices. Indeed, natural triples include (COC)–(FUEL)–(MTOW) variables taken separately for CENTRAL, LONG and SHORT design types. Corresponding plots are presented on Figures 5 and 6 for CENTRAL, LONG and SHORT designs.

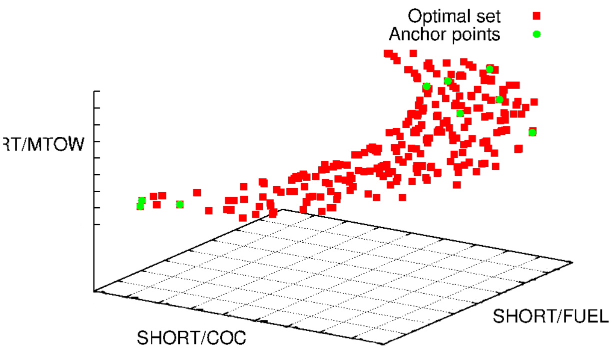

Figure 6: Pareto front projections onto coordinate triple (COC)–(FUEL)–(MTOW) for SHORT design type.

It is apparent that these front projections are very similar to analogous pictures of Pareto set. Indeed, everywhere Pareto front looks one-dimensional unless LONG/COC or SHORT/COC objectives are considered, see Figure 7. Once one of COC model responses for LONG or SHORT design types are taken into account Pareto front projection appears to be two-dimensional object which goes parallel to corresponding COC axis (see Figure 8). Moreover, inclusion of both LONG/COC and SHORT/COC objectives into projection makes Pareto front to look like three dimensional manifold, Figure 9.

Thus the plausible conclusion on the structure of Pareto front is similar to that of Pareto set. We clearly see that at fixed values of LONG/COC and SHORT/COC objectives Pareto front is essentially one-dimensional, while its dependence upon these distinguished responses is quite specific: front extends parallel to LONG/COC and SHORT/COC axes. Taking into account qualitatively identical behavior of Pareto set with respect to LONG/SLST and SHORT/SLST variables it is tempting to conclude that these four design variables and responses factually factorize. But of course, quantitative confirmation of this picture requires careful study of Pareto set/front interrelation which goes far beyond the capabilities of performed dumb analysis.

However, what we could quantitatively confirm is three-dimensional local structure of Pareto front. Indeed, we noted already that utilized multi-objective algorithm at its diffusion stage numerically determines local dimensionality via calculation of the eigenstructure of projected Gram matrix, see section 3. Hence we could reconstruct effective dimension of Pareto frontier by counting the number of non-zero eigenvalues. It turns out that in absolute majority of cases there are exactly three non-zero eigenvalues at locally Pareto optimal points. Deviation from this rule happens in less than 0.1% of cases and might be explained by pure numerical occasional instabilities.

4.2.1 Active Constraints

It remains to discuss the behavior of constraints on Pareto optimal solution set. Equalities are always active constraints and it turns out that they are indeed satisfied with great precision on all obtained solutions. As far as inequalities are concerned, direct inspection reveals that most of them are inactive on the Pareto set. However, this does not hold

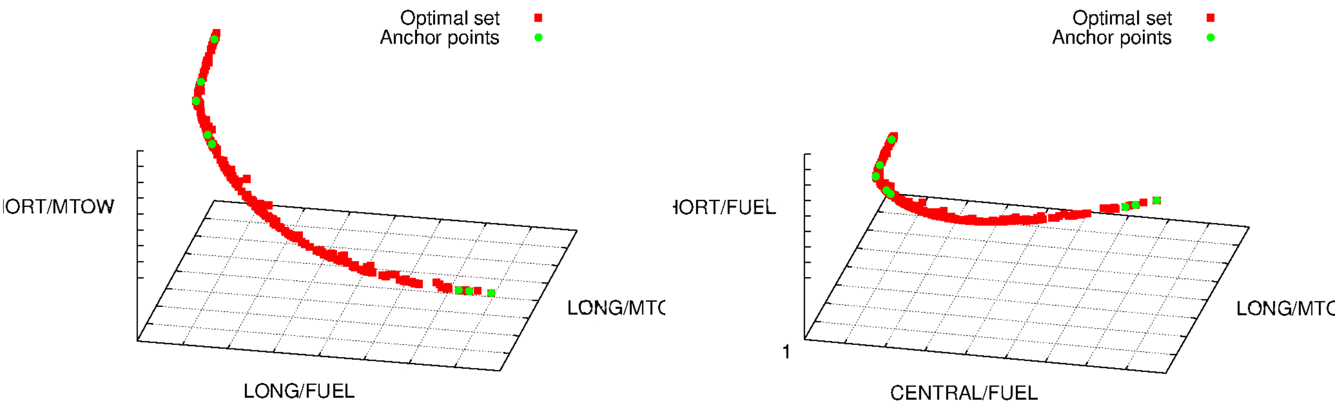

Figure 7: Pareto front projections onto various coordinate triples *excluding* LONG/COC and SHORT/COC objectives. Note that Pareto front looks one-dimensional.

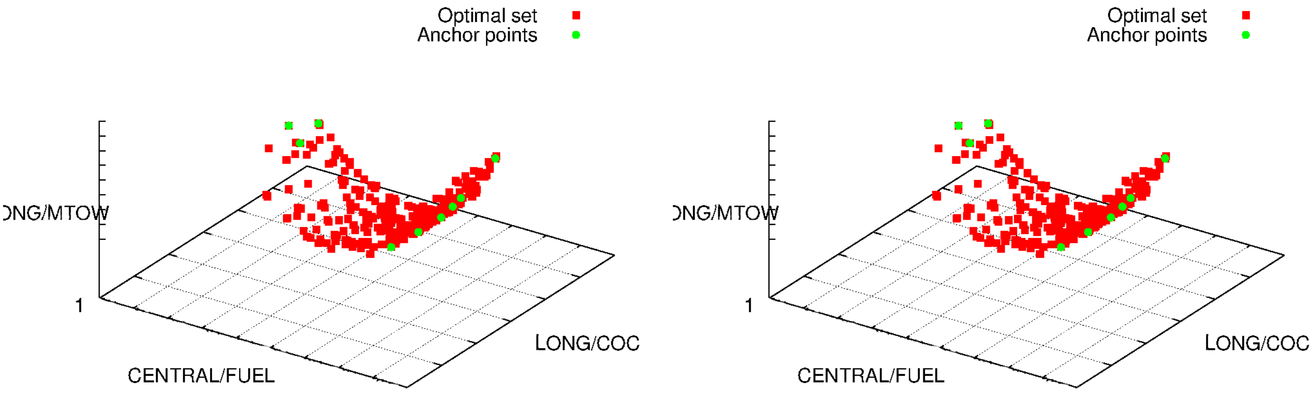

Figure 8: Pareto front projections onto various coordinate triples *including* either LONG/COC or SHORT/COC design variables. Note that Pareto front looks two-dimensional.

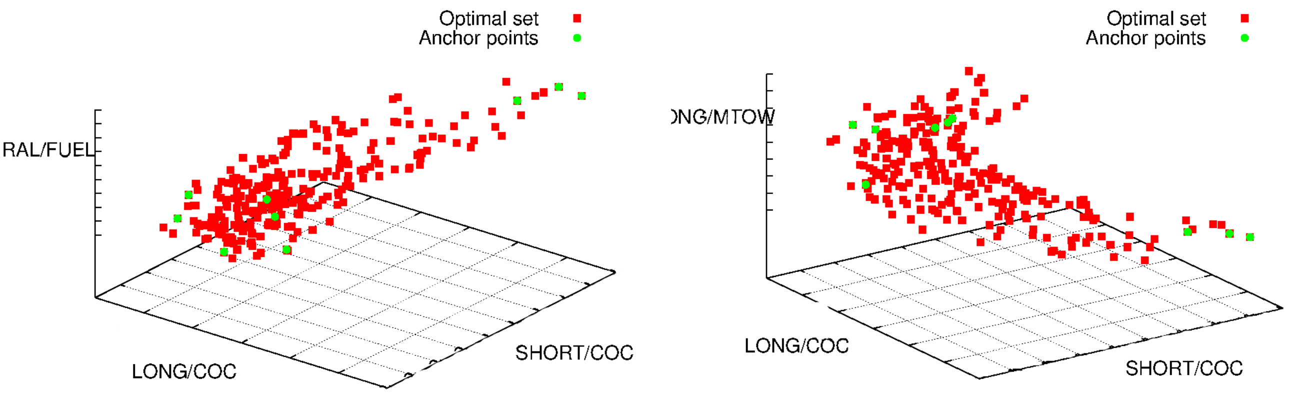

Figure 9: Pareto front projections onto various coordinate triples *including* both LONG/COC and SHORT/COC design variables. Note that Pareto front looks three-dimensional.

for two particular constraints of CENTRAL type. Although their magnitudes seems to be relatively large, they are nevertheless much smaller than characteristic scales. Thus we conclude that there are eight active constraints in the considered optimization problem. Amusingly enough, this nicely fits the three-dimensional structure of Pareto frontier. Indeed, we have originally 12 degrees of freedom (DoF), one of which (BPR) is fixed at upper box bound. Among remaining 11 DoF six are fixed by the equality constraints and 2 are eliminated by active inequalities. Therefore, there remains only 3 degrees of freedom which dictate established dimensionality of Pareto frontier.

4.3 Summary

We performed detailed quantitative analysis of obtained optimal solutions. Pareto set appears to be compact and is essentially three-dimensional. However, its embedding into the design space is very specific. Namely, it goes parallel to two distinguished coordinate axes, LONG/SLST and SHORT/SLST. At fixed values of these coordinates Pareto front seems to be one-dimensional. Pareto front inherits main properties of Pareto set. Namely, it appears to be also three-dimensional object, however, its embedding into objectives space is rather peculiar. It seems that Pareto front as a manifold is everywhere parallel to two objectives axes, LONG/COC and SHORT/COC. At fixed values of these observables Pareto front is likely to be one-dimensional non-linear curve embedded into $9 - 2 = 7$ dimensional space. The set of active constraints on Pareto optimal solutions seems to be small. Apart from "trivial" activity of all equalities there are only two active inequality constraints of CENTRAL design type.

5. Conclusions

In this paper we considered the problem of finding a set of optimal parameters governing conceptual design stage performances of family of aircrafts. This problem arises naturally in aerospace industry: production and operational costs are clearly minimal when different aircrafts have as much common components as possible, however, they target distinct market segments and hence must be sufficiently distinct. Quantitative treatment of these conflicting goals reduces to the solution of multi-objective constrained optimization problem, particular features of which include high dimensionality of objective space and large number of imposed constraints. Therefore, even with simplified underlying physical models for geometry, aerodynamics, weights and performances, the problem is quite challenging and, in fact, could not be solved with conventional methods.

Here the advantages of MACROS Generic Tool for Optimization [3] proved to be invaluable to exhaustively solve the problem. Using MACROS we were able to find not only the designs with greatly improved performances (from 10 to 20 percent), but to investigate the fine structure of Pareto Set and Front as well. It turns out that generic dimensionality of Pareto optimal variety is three, however, its embedding into design/performance criteria spaces is very peculiar: dependence upon two parameters/criteria essentially factorizes making Pareto set effectively one-dimensional object.

References

[1] J. Fliege, B.F. Svaiter, *"Steepest Descent Methods for Multicriteria Optimization"*, Mathematical Methods of Operations Research, 51(3), 2000, 479-494.

[2] J. Fliege, L.M.G. Drummond, B.F. Svaiter, *"Newton's Method for Multiobjective Optimization"*, SIAM J. Optim. 20(2), 2008, 602-626.

[3] DATADVANCE, http://www.datadvance.net